Chen *et al. Int J Concr Struct Mater* (2019) 13:10
https://doi.org/10.1186/s40069-018-0305-0

International Journal of Concrete Structures and Materials

RESEARCH Open Access

# Experimental Study and Analytical Modeling on Fatigue Properties of Pervious Concrete Made with Natural and Recycled Aggregates

Xudong Chen*, Dandan Shi, Nan Shen, Shengtao Li and Saisai Liu

**Abstract**

As a solid pollutant, the recycled aggregate can be reused to replace the natural aggregate to cast pervious concrete, promoting resource recycling and reducing environmental pollution. Pervious concrete is usually applied to transportation engineering as pavements and decks, which are often subjected to fatigue loads in service. Therefore, it is essential to investigate the fatigue mechanical properties of pervious concrete. In this study, four-point cyclic bending loading test of natural aggregate pervious concrete and recycled aggregate pervious concrete were conducted under four different stress levels. By analyzing the experimental results, the mechanical performances, including hysteresis curve characteristics, damping ratio, dynamic elastic modulus and cyclic strain, of two kinds of pervious concrete under cyclic loading were revealed. Based on the improved EPF model, the relationship between fracture parameters, plastic strain and unloading strain were obtained. Besides, the relationship between the loading cycles and the ratio of plastic strain to unloading strain was received according to fatigue testing data under different stress levels. Further, the simplified fatigue model of pervious concrete was proposed and the experimental data was fitted with the model results. The fitting result reached a good agreement.

**Keywords:** pervious concrete, recycled aggregate, fracture parameter, plastic strain, fatigue life prediction

## 1 Introduction

The lack of permeability of the pervious concrete pavement has brought great negative effects on the urban ecological environment, including urban waterlogging and traffic congestion (Joshaghani et al. 2015; Chandrappa and Biligiri 2016). Pervious concrete is a special material with high permeability by reducing the amount of fine aggregate in the concrete composition (Qin et al. 2015). The porosity of pervious concrete mainly depends on the aggregate gradation (Sumanasooriya and Neithalath 2011). At present, the most common application of pervious concrete is in the field of transportation engineering (Yang and Jiang 2003). Its special structure makes it not only have good air permeability and water permeability, but also have good ecological and environmental benefits such as temperature drop and noise reduction.

With the continuous aging of reinforced concrete buildings, together with the demolition and renovation of urban construction, more and more construction wastes are generated (Yehia et al. 2015). It is of great significance to use recycled building materials to develop pervious concrete reasonably and effectively so as to satisfy simultaneously requirements of high strength and good permeability. It is a solution to avoid two situations: removing construction waste and reducing the need of natural aggregate, preserving in both ways the natural resources (Thomas et al. 2014a). This is also the focus that scholars still need to study in the future (Senaratne et al. 2016).

The use of recycled aggregate instead of natural aggregate to prepare pervious concrete is conducive to the protection of natural environment and utilization of construction waste, which can bring huge economic and social benefits (Zhang et al. 2017; Fu et al. 2015). At present, scholars at home and abroad are still in the initial

*Correspondence: cxdong1985@hotmail.com
College of Civil and Transportation Engineering, Hohai University, Nanjing 210098, China
Journal information: ISSN 1976-0485 / eISSN 2234-1315

stage for the study of recycled aggregate pervious concrete. Bhutta et al. (2013) have studied the effect of recycled concrete aggregate on the permeability and strength of pervious concrete; Ćosić et al. (2015) have revealed the influence of aggregate type (dolomite or steel slag) and size (proportions of 4–8 mm to 8–16 mm aggregate fractions) on the properties of pervious concrete. Güneyisi et al. (2016) have investigated the effect of the replacement ratio of recycled aggregate and the ratio of water to cement on the mechanical properties of pervious concrete. The properties (compressive strength, density, total void, water permeability, thermal conductivity and surface abrasion resistance) of pervious concretes made with recycled concrete block aggregate and recycled concrete aggregate were studied by Zaetang et al. (2016). Barnhouse and Srubar (2016) investigated the mechanical, physical and hydraulic conductivity properties of pervious concrete containing recycled aggregates.

The research conducted so far has mainly focused on the effects of the type and substitution rate of recycled aggregate on the permeability and mechanical properties of pervious concrete (Sriravindrarajah et al. 2012; Güneyisi et al. 2016; Zhang et al. 2017). However, pervious concrete is often applied to transportation engineering, which is usually subjected to fatigue load (Li and Yu 2014; Mannan et al. 2015). Arora and Singh (2016) investigated the flexural fatigue performance of concrete beams made with 100% coarse recycled concrete aggregates (RCA), which were also compared with that of concrete made with 100% coarse natural aggregates (NA). Xiao et al. (2013) conducted the uniaxial compression tests to calculate and analyze the residual strain variation, the fatigue strain variation and the fatigue modulus of recycled aggregate concrete. Thomas et al. (2014b) carried out the research to obtain the fatigue limit of recycled aggregate concrete with different aggregated replacements and water/cement ratios. Recycled aggregate concretes produced with partial and total coarse aggregate replacement and control concretes with different water/cement ratios have been cast to study the material's behavior in response to repeated compressive loads using the Locati method by Thomas et al. (2014a, b). Heeralal et al. (2009) studied the influences of the different replacements of recycled aggregate in natural aggregate, presence of steel fiber and different stress levels on the flexural fatigue behavior of steel fiber reinforced recycled aggregate concrete. But there is very limited research undertaken in regard with the fatigue performance of previous concrete with recycled aggregate. Therefore, it is of great importance to study the fatigue mechanical properties of pervious concrete.

In this study, four-point cyclic bending loading tests for natural aggregate pervious concrete (NAPC) and recycled aggregate pervious concrete (RAPC) were carried out under four different stress levels. Area of hysteresis loop, damping ratio, dynamic elastic modulus, and cyclic strain of NAPC and RAPC under fatigue loading were investigated and compared. Meanwhile, the elasto-plastic and fracture (EPF) model (Maekawa and Okamura 1983) was improved to establish the relationship between the fracture parameters, the plastic strain and the unloading strain. And then the static stress–strain models of the pervious concrete can be obtained. Through the experimental data analysis and fitting, the relationship curves between the loading cycles and the ratio of plastic strain to unloading strain of pervious concrete were obtained under different stress levels. On this basis, the simplified fatigue model of pervious concrete under bending cyclic loading was proposed to evaluate the variations of mechanical properties and predict the fatigue life of pervious concrete specimens at different stress levels. The prediction results of the model are well fitted with the test results.

## 2 Experimental Work

### 2.1 Materials and Mix Proportions

The ordinary Portland cement with grade 42.5 was used as the cementitious materials for the pervious concrete specimens. The natural aggregate was basalt with a maximum particle size of 15 mm, as shown in Fig. 1a. The recycled aggregates with the size of 10–15 mm were obtained by crushing and sifting the abandoned concrete blocks as shown in Fig. 1b. The main physical properties of natural and recycled aggregates are given in Table 1. The additive is a mixture of polycarboxylic acid superplasticizer and granulated blast furnace slag. Water was the tap water from laboratory. The mix proportions of pervious concrete made with two different aggregates are shown in Table 2. The dimensions of the specimens are 100 mm × 100 mm × 400 mm.

### 2.2 Molding and Curing of Specimen

In order to mix the materials evenly, the first step was to add the cement, additive and aggregates, weighed according to the mix proportion, to the mixer and stirred for 25 s. Then 50% of the total water was added with stirred for 35 s to make the mixture reach a uniform wet state. Finally, the remaining water and admixture were added together and the time of stirring in the final stage was about 120 s.

When the fresh pervious concrete was moulded, both the tamping and vibrating methods were used in the study. The tamping rod was utilized to tamp the fresh pervious concrete for 3 times in the procedure when the material reached 1/3, 2/3 and all of the mould volume. Then the mould was put onto the vibrating table for 5 s of vibration, after which the surface was carefully smoothed

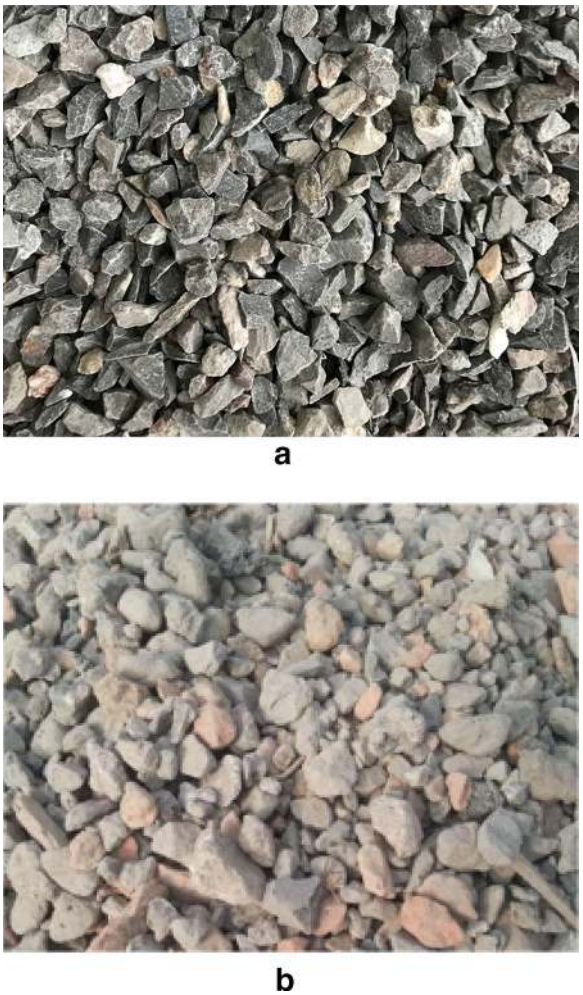


**Fig. 1** Aggregates: **a** natural aggregates and **b** recycled aggregates.

**Table 1 Main physical properties of natural and recycled aggregates.**

| Type | Density (kg/m$^3$) | Water absorption (%) | Crushing value (%) |
|---|---|---|---|
| Natural aggregate | 2752 | 1.12 | 4.00 |
| Recycled aggregate | 2633 | 3.25 | 13.42 |

**Table 2 Mix proportions for pervious concrete (kg/m$^3$).**

| | Cement | Water | Aggregate | Additive | *w/c* |
|---|---|---|---|---|---|
| NAPC | 368 | 110 | 1425 | 23.4 | 0.30 |
| RAPC | 368 | 110 | 1363 | 23.4 | 0.30 |

1.0 kg = 2.2046 lb; 1.0 m = 3.281 ft.

by a steel disc. When the moulding process was finished, all the specimens were immediately coated with a plastic membrane which had been brushed with oil to minimize the influence of water evaporation on cement hydration and strength growth. Demoulding started as soon as the specimens were cured in the curing room for 24 h, and then the specimens were cured by the method of sprinkling water until the 28 days age was reached.

### 2.3 Loading Method

In this study, the tests included three parts: quasi-static monotonic four-point bending tests, quasi-static four-point loading–unloading bending tests and four-point cyclic bending tests under four high-stresses. The detailed descriptions of the three tests are as followings.

1. The quasi-static monotonic four-point bending test was conducted with three specimens selected from pervious concrete for each type of aggregates. The control mode was load control. The loading rates were 100 N/s.
2. Two specimens made with different aggregates were used in the quasi-static four-point bending test. The loading–unloading test was carried out when the strain increased by 50 με in the period of pre-peak and 200 με in the period of post-peak.
3. The average value of maximum loads obtained from the quasi-static tests was taken as the peak load. And the four-point bending tests were carried out at 90, 85, 80 and 75% of the peak load, respectively. The loading waveform is shown in the Fig. 2. The loading frequency was 1 Hz. In order to ensure that continuous contact was maintained between the loading head and the specimen during the fatigue test, the minimum load was determined to be 0.5 kN. The specimen and the test setup are presented in Fig. 3.

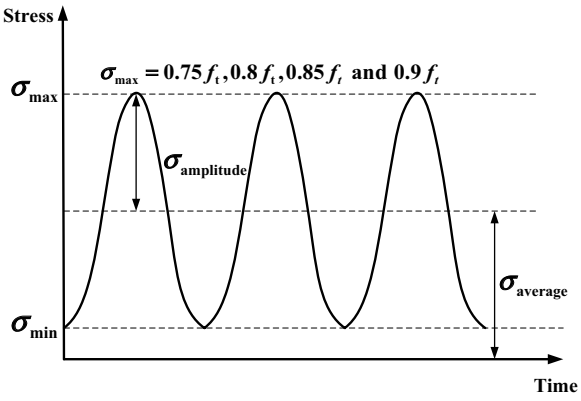


**Fig. 2** Loading waveform.

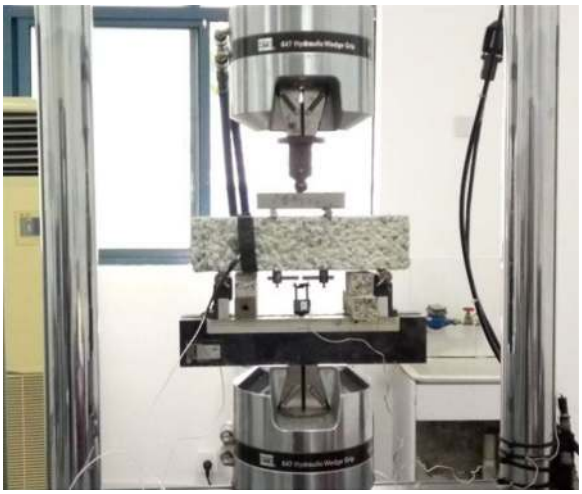

**Fig. 3** Four-point bending test setup MTS810.

## 3 Experimental Results and Analysis

### 3.1 Static Bending Strength

The strengths of pervious concrete specimens made with two different aggregates are shown in Table 3. It can be seen that the strength of NAPC significantly higher than that of RAPC. There are two main reasons for this phenomenon. On one side, micro-cracks emerged in the crushing process of recycled aggregates, which made the mortar attached to the aggregate loose. As a result, the porosity increased and the strength of aggregate decreased. On the other side, weak interface inevitably existed between old and fresh cement paste on the surface of recycled aggregates due to the weak cohesion.

**Table 3 Static four-point bending strength for pervious concrete (MPa).**

| No. | NAPC | RAPC |
|---|---|---|
| 1 | 4.01 | 3.26 |
| 2 | 4.23 | 3.08 |
| 3 | 4.21 | 3.35 |
| Average | 4.15 | 3.23 |

### 3.2 Failure Mode

The failure mode of the specimen under four-point bending loading is presented in Fig. 4. As can be seen from the figure, the NAPC and RAPC specimens were both broken in the maximum bending moment zone. The average aggregate size of recycled aggregates is larger. Besides, recycled aggregates are more angular than natural aggregates. Therefore, there are more internal micro-cracks inside of the RAPC specimens.

### 3.3 Hysteresis Loop

If the specimen is an ideal elasto-plastic body, the curves of stress–time and strain–time should be unified in time (Chen et al. 2017). That is to say, when dynamic stress acts, dynamic strain arises. However, the pervious concrete is non-ideal elasto-plastic body because of the micro-structural characteristics such as cracks, holes and contact surfaces, which make the stress–strain curve form a hysteresis loop for the same loading cycle.

The typical hysteresis loop is drawn as Fig. 5. In the cyclic loading–unloading test, when the external load

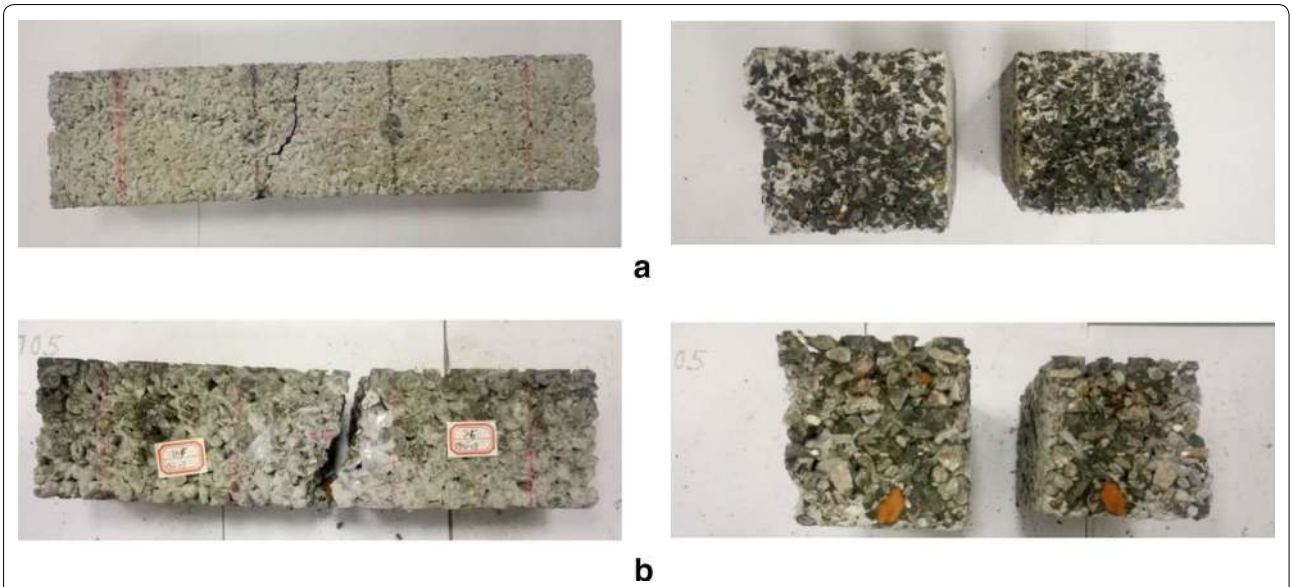


**Fig. 4** Failure mode: **a** NAPC and **b** RAPC.

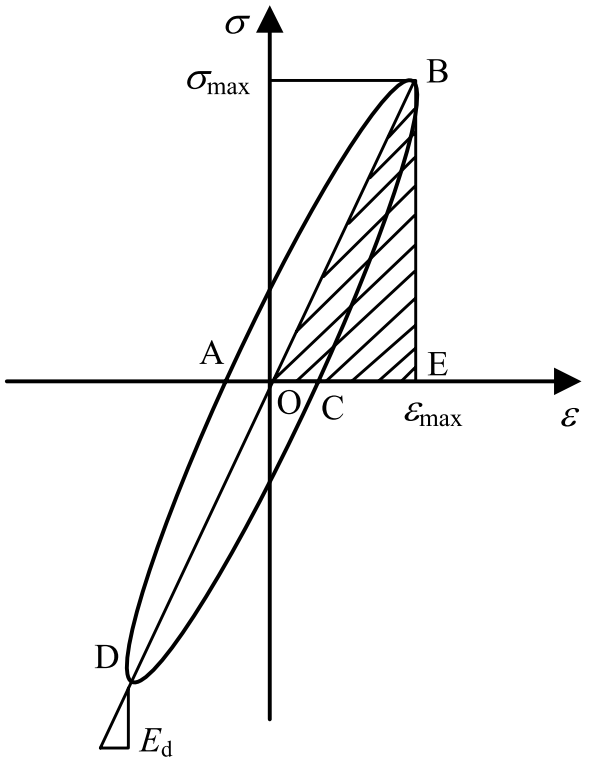


**Fig. 5** Sketch of hysteresis loop.

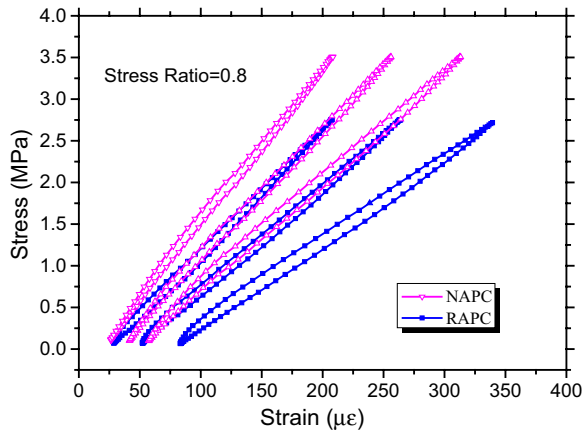


**Fig. 6** Hysteresis loop under different cycle ratio at stress level of 0.8.

reverses, the greater the plastic deformation is, the more hysteretic the elastic deformation responds. At this point, the stress–strain hysteresis loop is more like an oval. By contrast, the hysteresis loop is more like the shape of the sharp leaf. The stress–strain hysteresis loops of the two mixes are shown in Fig. 6 at the stress level of 0.8. It can be seen that the hysteresis curves of two mixes are similar to the shape of the sharp leaf. The hysteresis curves of NAPC are sharper when the load reverses, which indicates that the elastic deformation of NAPC specimens recovers quickly and the plastic strain is small at this time.

The area of the hysteresis loop reflects the energy dissipation during the loading–unloading process, which indicates the extent of the opening and closing of the micro cracks under cyclic loading. The larger the area of the hysteresis loop is, the more the dissipation energy and the greater the damage caused by the cyclic loads become.

As listed in Table 4, the areas of hysteresis loops for pervious concrete specimens at the cycle ratio of 0.1, 0.5 and 0.9 are presented. The cycle ratio is defined as the ratio of the number of cycles $N$ to the fatigue life $N_f$, which is used to analyze the fatigue characteristics.

According to the data in Table 4, it can be seen that with the increase of the cycle ratio, the hysteresis loop

**Table 4 Areas of hysteresis loop at different stress levels (Pa).**

| Groups | Stress levels | Cycle ratios | | |
|---|---|---|---|---|
| | | 0.1 | 0.5 | 0.9 |
| NAPC | 0.75 | 9.12 | 11.62 | 12.67 |
| | 0.8 | 11.49 | 12.32 | 15.16 |
| | 0.85 | 23.68 | 28.74 | 43.42 |
| | 0.9 | 46.01 | 58.07 | 130.50 |
| RAPC | 0.75 | 7.90 | 12.58 | 17.13 |
| | 0.8 | 14.03 | 18.59 | 31.40 |
| | 0.85 | 21.82 | 28.09 | 42.28 |
| | 0.9 | 23.22 | 33.19 | 69.21 |

of the specimen gradually moves towards the direction of strain increase. This states that the damage of specimen caused by irreversible deformation is becoming larger as the number of loading cycle increases. When the stress level is low, the plastic strain developed rapidly in the initial stage of cyclic loading, resulting from pores and the micro-cracks from hydration reaction inside concrete specimen. With the increase of stress level, the friction between components of pervious concrete is relatively strong, resulting in an increase in energy consumption. Thus, the area of the hysteresis loop and the plastic deformation both gradually increase.

### 3.4 Damping Ratio

The calculation formula of the damping ratio is presented as following:

$$\lambda = A_h / (4\pi A_s) \quad (1)$$

where $A_h$ represents the area of the hysteresis loop $ABCDA$, and $A_s$ represents the area of the triangle $OAE$,

**Table 5 Damping ratios at different stress levels (%).**

| Groups | Stress levels | Cycle ratios | | |
|---|---|---|---|---|
| | | 0.1 | 0.5 | 0.9 |
| NAPC | 0.75 | 1.08 | 1.27 | 1.29 |
| | 0.8 | 1.45 | 1.53 | 1.64 |
| | 0.85 | 2.46 | 2.52 | 3.11 |
| | 0.9 | 3.47 | 3.79 | 5.8 |
| RAPC | 0.75 | 1.39 | 1.77 | 2.05 |
| | 0.8 | 1.67 | 2.01 | 2.74 |
| | 0.85 | 2.36 | 3.17 | 4.02 |
| | 0.9 | 3.07 | 3.58 | 4.75 |

as shown in Fig. 5. The damping ratios of NAPC and RAPC are calculated by using the data at the cycle ratios of 0.1, 0.5, 0.9, respectively.

The results are listed in Table 5. It is easy to know that the damping ratio of the pervious concrete specimen increases with the increase of the cyclic stress levels and the number of cycles. For the specimens under larger cyclic loads, the deformation is greater and the friction between aggregates inside the specimen is more intense. Then the interfacial bonding becomes weaker. As a result, the damping ratio of specimens increases.

The interface cohesion of coarse aggregate significantly affects the damping ratio of concrete. Therefore, comparing NAPC to RAPC, the latter has higher damping ratio because of weak internal connection caused by weak and cracked mortar attached to the surface. This can also be proved according to the data in Table 5.

### 3.5 Dynamic Elastic Modulus

The slope of the hysteresis loop is defined as the dynamic elastic modulus. As shown in Fig. 5, the formula can be expressed as following:

$$E = \sigma_{\max} / \varepsilon_{\max} \quad (2)$$

where $\sigma_{\max}$ represents the maximum stress, $\varepsilon_{\max}$ represents the maximum strain.

According to the experimental data, the dynamic elastic modulus of two different aggregate pervious concrete under different stress levels can be calculated.

As depicted in Fig. 7, the internal cracks develop more fully with the increase of loading cycles, which results in a larger damage and the decrease of dynamic elastic modulus. The dynamic elastic modulus presents a three-stage degradation law. It decreases faster within the 10% of the cycle ratio, and descends slowly in the second stage. The decline ratio increases when the cycle ratio is up to 0.8.

In Fig. 7, it can also be seen that the dynamic elastic modulus of the specimen decreases by about 30–40%

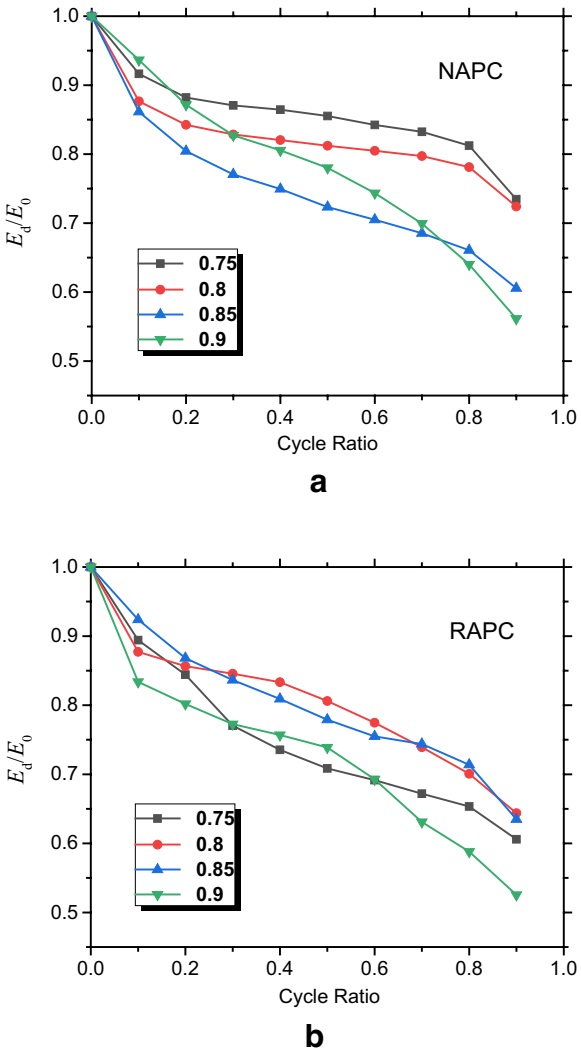


**Fig. 7** The variation of $E_d/E_0$ at different cycle ratios under four stress levels: **a** NAPC and **b** RAPC.

before the failure of the pervious specimen under the cyclic load. Comparing Fig. 7a, b, it can be found that the dynamic elastic modulus of RAPC decreases more quickly and the residual dynamic elastic modulus of RAPC is lower than that of NAPC. This may be due to the greater internal damage of RAPC under the cyclic loads because of the weak bond between the old mortar on the surface of the recycled aggregate and the new cement paste, which leads to a sharp decrease in its bearing capacity.

### 3.6 Total and Plastic Strains

The total strain is the axial strain at the maximum stress after a certain number of loading cycles. And the plastic strain is the unrecoverable deformation of a specimen

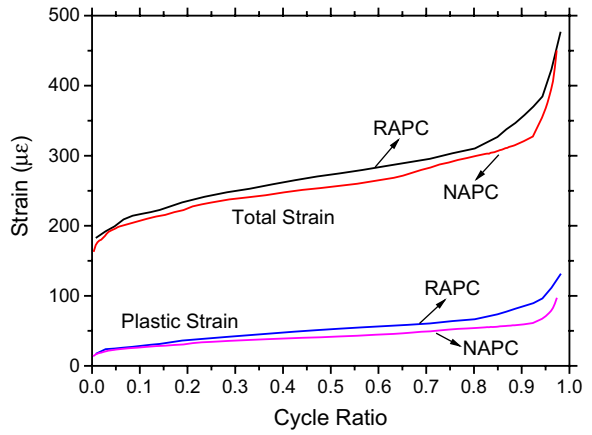


**Fig. 8** Variations curves of total strain and plastic strain at stress level of 0.8.

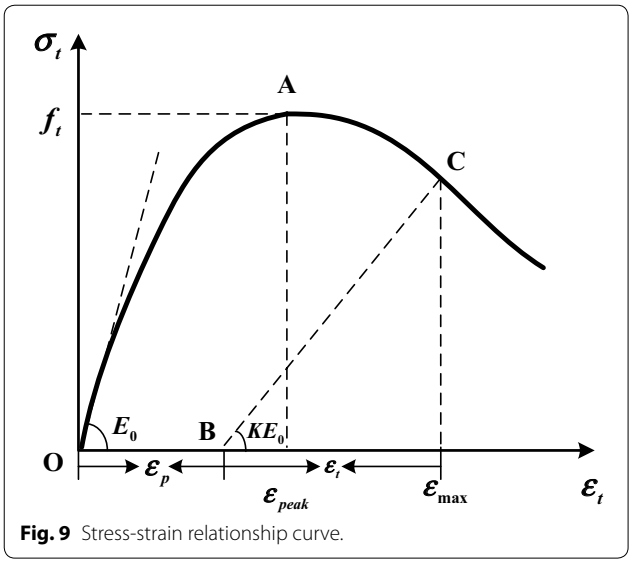


**Fig. 9** Stress-strain relationship curve.

when the stress is unloaded to the zero, which is determined by the line connecting the total strain at the maximum stress and the strain at the minimum stress.

When the stress level is 0.8, the change curves of total strain and plastic strain of NAPC and RAPC specimens during cyclic loading are shown in Fig. 8. The obvious three-stage trend can be indicted from the curves in Fig. 8. In the 5% of fatigue life, the total strain and the plastic strain both increase rapidly because of the initial development of micro-cracks and the existed defects inside of the specimens. The second stage is about 5–90% of the fatigue life. Strain increases at a low rate at this stage because of the development of new micro-cracks and the tensile creep of samples under cyclic loading. After that, the micro-cracks rapidly connect to form macroscopic cracks, resulting in a rapid increase of the strain. This is the third stage of strain development, which is in the last 5% of fatigue life.

In Fig. 8, it can also be seen that the plastic strain and the total strain of the RAPC are greater than that of the NAPC under the same cycle ratio. This is because of the high crushing value of the recycled aggregate, which results in that the recycled aggregates are easily broken under loading and occur mutual dislocation. Therefore, the recycled aggregate pervious concrete specimens are more likely to fail, with the unrecoverable deformation and the cracks becoming larger and wider.

## 4 Fatigue Life Prediction Model

In this study, the stress–strain relationship of two different aggregate pervious concrete is proposed, which is based on the elasto-plastic and fracture model (EPF) of concrete proposed by Maekawa and Okamura (Maekawa and Okamura 1983). In the EPF model, the stress–strain relationship is shown in Fig. 9 and can be expressed as Eq. (3).

$$\sigma = KE_0(\varepsilon_{\max} - \varepsilon_{\mathrm{p}}) \tag{3}$$

where $\sigma$ is stress, $\varepsilon_{\max}$ is the unloading strain. $\varepsilon_{\mathrm{p}}$ is the plastic strain. $K$ represents the fracture parameter. $E_0$ represents the Young's modulus. The fracture parameter $K$ and the plastic strain $\varepsilon_{\mathrm{p}}$ are both the functions of the unloading strain $\varepsilon_{\max}$ and the peak strain $\varepsilon_{\mathrm{peak}}$.

Because of the absence of fine aggregates in the pervious concrete, the mechanical properties of the specimens such as strength, stiffness and deformation, are different from those of ordinary concrete specimens subjected to loads. Therefore, the functions of fracture parameters and plastic strain in the EPF model are no longer applicable and need to be improved. In order to obtain the variations of the stiffness and the plastic strain, static unloading–reloading tests were conducted on the two types of pervious concrete.

The static loading–unloading curves for two different aggregates pervious concrete are drawn in Fig. 10. According to the experimental data, the EPF model was modified to obtain the relationship between the fracture parameter $K$, the plastic strain $\varepsilon_{\mathrm{p}}$ and the unloading strain $\varepsilon_{\max}$. The initial elastic modulus and peak strain of the two aggregates pervious concrete are shown in Table 6.

### 4.1 Fracture Parameter

In Fig. 8, the curve slope of the point O is defined as the initial Young's modulus $E_0$. And the connection between the unloading point C and the minimum stress point B is defined as the secant modulus. In this study, the fracture parameter $K$ is defined as the ratio of the secant modulus at a certain loading cycles to the Young's modulus $E_0$ of the pervious concrete specimen. It represents the degree

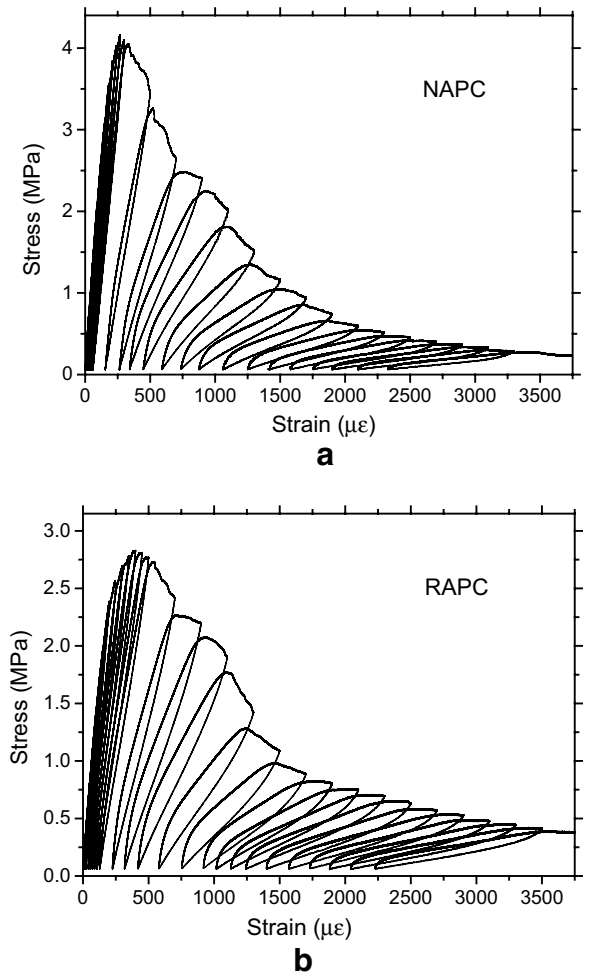


**Fig. 10** Stress-strain curves during loading–unloading process for pervious concrete: **a** NAPC and **b** RAPC.

of internal damage of specimen under loading. According to the experimental data obtained from static unloading–loading test, the values of fracture parameter $K$ of pervious concrete made with two kinds of aggregates at different stress levels are calculated, and the relationship can be expressed as Eq. (4).

$$K = \exp\left\{-a_1\varepsilon_{\max}\left(1 - \exp\left(-b_1\frac{\varepsilon_{\max}}{\varepsilon_{peak}}\right)\right)\right\} \tag{4}$$

The experimental data were used to calculate by Eq. (4). The values of parameters $a_1$ and $b_1$ are obtained and shown in Table 7.

The value of the fracture parameter $K$ calculated from experiment and the fitting curve obtained by proposed model are both drawn in Fig. 11. The curve fits well with the experimental results.

**Table 6 Elastic modulus and peak strains of different aggregate pervious concretes.**

| Group | Elastic modulus/GPa | Peak strain/με |
|---|---|---|
| NAPC | 24.880 | 265.88 |
| RAPC | 18.228 | 379.93 |

**Table 7 Fitting values of parameter $a_1$ and $b_1$.**

| Group | $a_1$ | $b_1$ | $R^2$ |
|---|---|---|---|
| NAPC | | | |
| Pre-peak | 0.005 | 0.27 | 0.99 |
| Post-peak | 0.002 | 0.95 | 0.99 |
| RAPC | | | |
| Pre-peak | 0.0017 | 1.75 | 0.98 |
| Post-peak | 0.0017 | 2.5 | 0.99 |

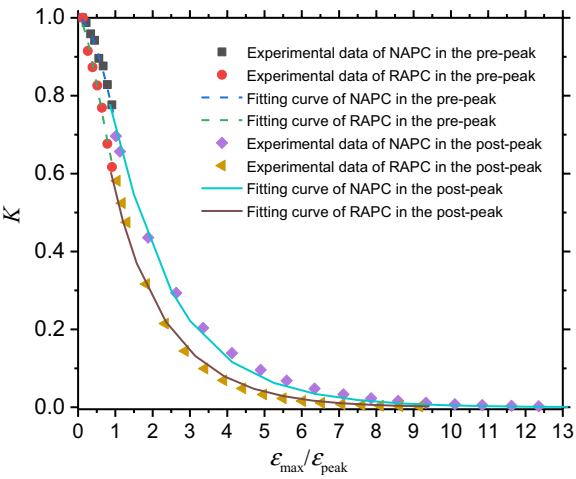


**Fig. 11** Fitting curve of fracture parameter.

As presented in Fig. 11, the fracture parameter decreased obviously before the peak. And the descend trend gradually becomes gentle as the ratio of $\varepsilon_{\max}$ to $\varepsilon_{\text{peak}}$ increases. When the value of $\varepsilon_{\max}/\varepsilon_{\text{peak}}$ is more than 5, the value of the fracture parameters is declined to less than 0.1 for both NAPC and RAPC. Besides, the fracture parameters of RAPC are obviously less than those of NAPC at the same ratio of $\varepsilon_{\max}$ to $\varepsilon_{\text{peak}}$. This is because the bond of mortar and coarse aggregate in recycled aggregate concrete is weak, which cause the relatively bigger slippage in the interfacial transition zone. Thus, the bearing capacity of RAPC specimen decrease rapidly and specimens are easy to fracture.

### 4.2 Plastic Strain

The deformation of brittle materials includes plastic deformation (irreversible deformation) and elastic deformation. In the cyclic loading, the elastic deformation is restored when the load removes while the plastic deformation remains. The plastic deformation is directly related to the degree of material damage, which reflects fatigue performance of concrete under cyclic loading.

Similar to the fracture parameter, the equation of plastic strain can be obtained from the experimental data, as shown in Eq. (5).

$$\varepsilon_p = \varepsilon_{\max} - a_2\varepsilon_{peak}\left\{1 - \exp\left(-b_2\frac{\varepsilon_{\max}}{\varepsilon_{peak}}\right)\right\} \tag{5}$$

The values of parameter $a_2$ and $b_2$ are listed in Table 8. The relationship curves between the plastic strain and the ratio of $\varepsilon_{\max}$ to $\varepsilon_{\text{peak}}$ are depicted in Fig. 12. Under the loads, the plastic strain of the pervious concrete specimen increases slowly when the unloading strain is less than peak strain. However, when the peak strain is reached, the plastic strain increases rapidly until the sample fails.

**Table 8 Fitting values of parameter $a_2$ and $b_2$.**

| Group | $a_2$ | $b_2$ | $R^2$ |
|---|---|---|---|
| NAPC | | | |
| Pre-peak | 2.86 | 0.35 | 0.99 |
| Post-peak | 4.04 | 0.23 | 0.99 |
| RAPC | | | |
| Pre-peak | 1.78 | 0.57 | 0.99 |
| Post-peak | 4.04 | 0.20 | 0.99 |

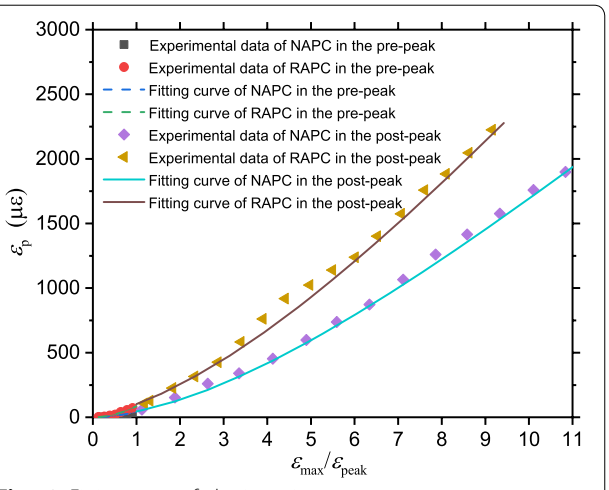


**Fig. 12** Fitting curve of plastic strain.

Comparing the two mixes, larger plastic strain can be found in RAPC specimens at the same ratio of $\varepsilon_{\max}$ to $\varepsilon_{\text{peak}}$. When the value of $\varepsilon_{\max}/\varepsilon_{\text{peak}}$ is greater than 1, the variation rates of plastic strain for both NAPC and RAPC increase rapidly. Besides, the difference between the plastic strains of two mixes increase with the increase of $\varepsilon_{\max}/\varepsilon_{\text{peak}}$. Due to the existance of many initial micro-cracks and pores inside the RAPC specimens, the cracks in the specimen extended and interconnected more easily under the continuous loading, which results in larger irreversible damage (plastic strain) of specimens.

### 4.3 Loading Cycles

The relationship between the ratio of plastic strain $\varepsilon_{\text{p},Ni}$ to maximum strain $\varepsilon_{\max,Ni}$ and the logarithm of loading cycle $\log N_i$ is formulated on the basis of experimental data in the cyclic loading tests at different stress levels, as expressed in Eq. (6).

$$LogN_i = A\left(1 - \exp\left(-B\frac{\varepsilon_{p,Ni}}{\varepsilon_{\max},Ni}\right)\right) - C \tag{6}$$

Here, parameter A, B and C are the function of normalized maximum stress level and can be calculated using the equations listed in Table 9. It can be found that the experimental data are close to that in the calculated curves.

From Fig. 13, it can be seen that for the same type of pervious concrete, the ratio of the plastic strain to the maximum strain at failure becomes larger with the increase of stress level under fatigue loading. The reason may be that the fatigue life indicated by the loading cycles is larger when the stress level is low, which makes the internal micro-cracks more fully developed and increases the plastic strain in the long-time cyclic loading. Comparing Fig. 13a with Fig. 13b, it can also be seen that the plastic strain of RAPC at failure is larger than that of NAPC under the same stress level, which is in accordance with the conclusion drawn in Sect. 4.2. Moreover, it can be concluded that the fatigue life of RAPC is lower than that of NAPC, and the reason may be explained that the fatigue properties of RAPC is more sensitive to the initial defects inside RAPC specimens such as pores and micro-cracks which are more likely to develop under flexural tensile stress.

**Table 9 Fitting curves of parameter A, B and C.**

| Group | Parameters | | |
|---|---|---|---|
| | A | B | C |
| NAPC | $15.00/(1.20S_{\max})^{-11.6}$ | $11.6\,(1.25S_{\max})^{5.7}$ | $(1.37S_{\max})^{16.5}$ |
| RAPC | $10.85/(1.25S_{\max})^{-7.0}$ | $19.0\,(1.15S_{\max})^{2.5}$ | $(1.50S_{\max})^{10.5}$ |

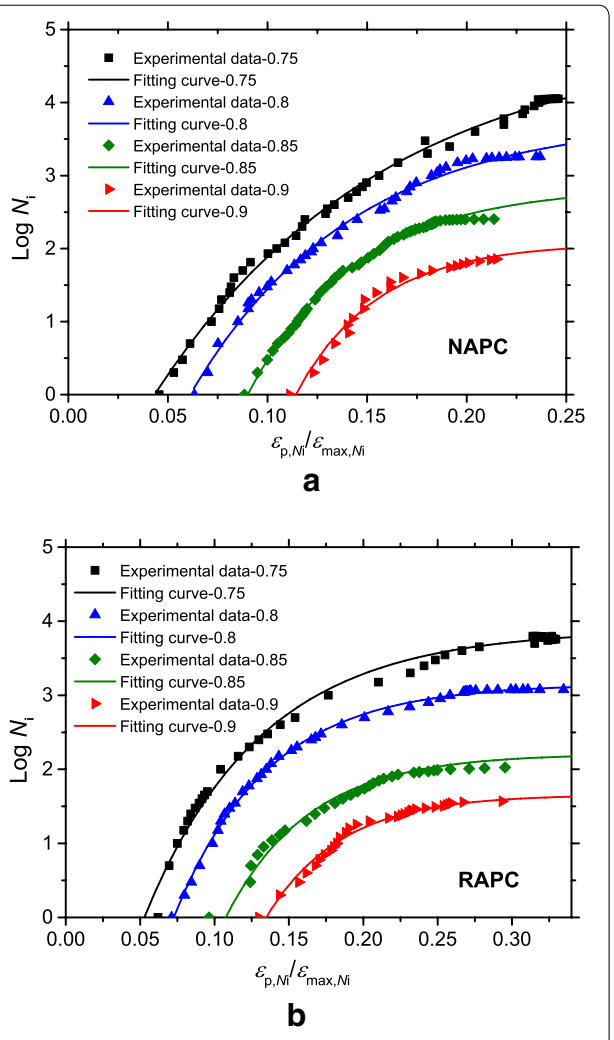


**Fig. 13** Fitting curve of fatigue life for pervious concrete: **a** NAPC and **b** RAPC.

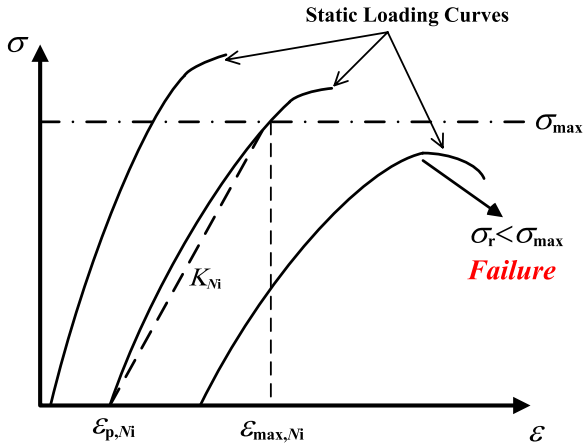


**Fig. 14** A diagram for failure criterion.

### 4.4 Simplified Fatigue Model

In the previous researches, to consider the non-linearity (El-Kashif and Maekawa 2004) of concrete and evaluate the fatigue life (Maekawa et al. 2006) of damaged concrete structures under cyclic loading, the fatigue life prediction models based on time and deformational paths are mainly dependent on similar elasto-plastic and fracture model theories.

In this part, the static stress–strain model of pervious concrete based on EPF model is extended to propose the simplified fatigue model. It can not only assess the variations of total strain, plastic strain and fracture parameter of pervious concrete at respective number of loading cycle, but also predict the fatigue life of pervious concrete under different stress levels.

In order to predict the fatigue life of pervious concrete specimens under cyclic loading, a failure criterion needs be settled. In this research, the residual strength of specimen is determined, which is equal to the peak stress calculated by the stress–strain relationship shown in Eq. (3). As presented in Fig. 14, when the residual strength is lower than the applied maximum stress, it means that the pervious concrete specimen fails.

Figure 15 presents the flow chart to evaluate the fracture parameters and predict fatigue life. It should be noted that the values of $\varepsilon_{max,1}$ and $\varepsilon_{peak}$ need to be compared to choose the right values of parameters. In the first step, the basic parameters, including flexural strength, initial modulus and peak strain, are obtained according to the static monotonic test. The stress–strain curve can be drawn by using the static stress–strain model of pervious concrete based on the EPF model. Then the maximum strain $\varepsilon_{max,1}$ is calculated using the proposed static stress–strain model with the maximum applied stress. Thereafter, the unloading strain, that should be larger than $\varepsilon_{max,1}$, for the first cycle of loading–unloading is given. And the corresponding fracture parameter and plastic strain are calculated using the Eqs. (4) and (5). Next, the number of cycles ($N_i$) can be obtained for $\varepsilon_{p,Ni}/\varepsilon_{max,Ni}$ using the Eq. (6).

The fracture parameter and the plastic strain calculated in the previous step are introduced into Eq. (3) to determine the residual strength $\sigma_r$. In order to judge whether the specimen fails or not, the residual strength is compared with the maximum applied stress. If the former is less than the latter, the specimen fails and the number of cycles at this time is the fatigue life of the pervious concrete specimen. If the residual strength is greater than the maximum applied stress, the calculation step need to be

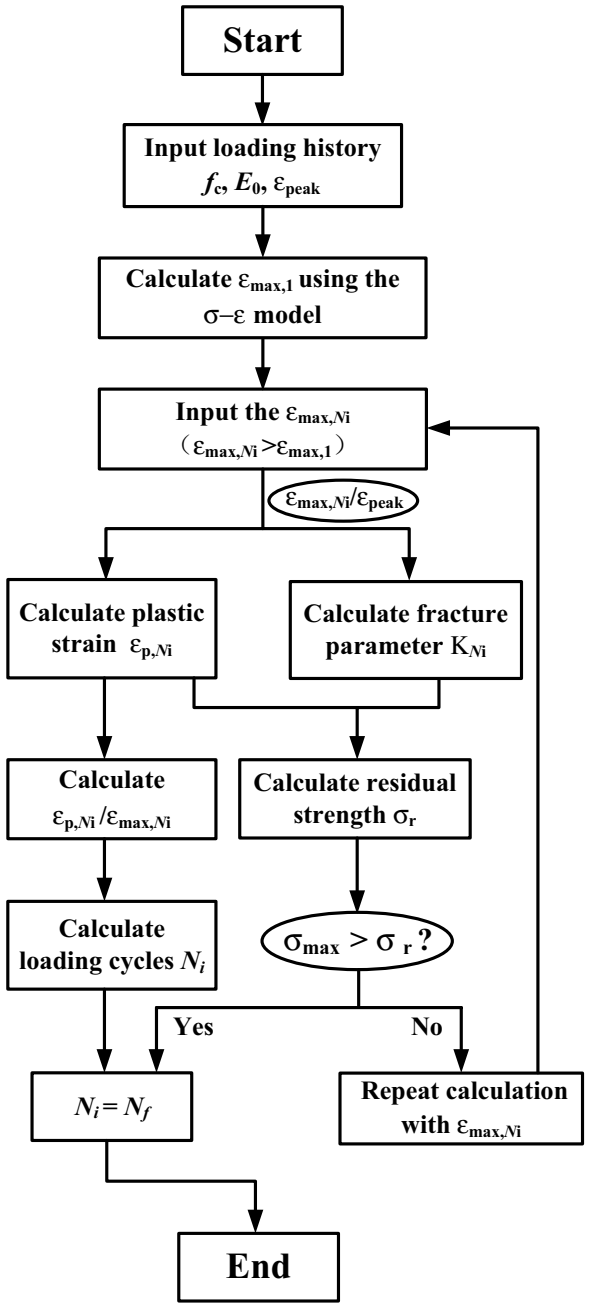


**Fig. 15** Flow chart of simplified fatigue model.

repeated with the next $\varepsilon_{max,\,Ni}$ until the residual strength of the pervious concrete is less than the maximum applied stress.

### 4.5 Model Validation

Using the simplified fatigue model proposed in the Sect. 4.4, the experimental data of NAPC and RAPC were tested at a stress level of 0.85.

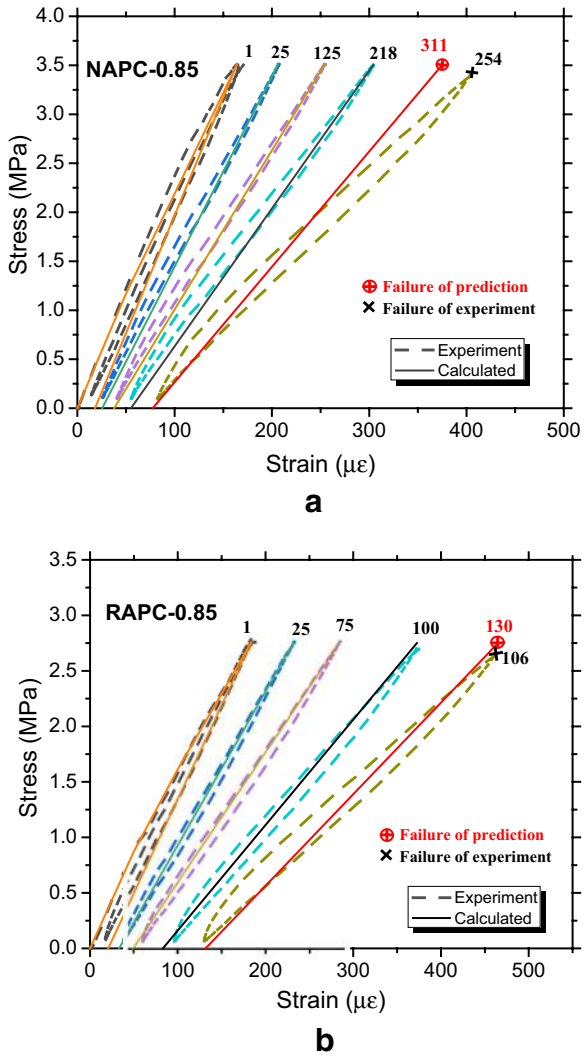


**Fig. 16** Model verification under the stress level of 0.85: **a** NAPC and **b** RAPC.

The fracture parameters and the plastic strain were calculated. On this basis, the fatigue lives of NAPC and RAPC under cyclic loading were predicted. When the stress level is 0.85, the fatigue life obtained from tests of NAPC and RAPC are 254 and 105, respectively, while the fatigue life calculated according to the proposed model are 311 and 130, respectively. The results of model validation are shown in Fig. 16. Comparing with Fig. 16a, b, it is worth noting the plastic strain of recycled aggregate pervious concrete is larger and the dynamic elastic modulus are down even more when the specimens fails, which is also consistent with the conclusion of the previous chapter in this paper.

In general, the calculated results are in good agreement with the experimental results. The model can effectively

evaluate the changes of the basic physical properties of the pervious concrete and predict its fatigue life under cyclic loads. But the experimental data in other literatures can be used to validate the model are seldom seen. Therefore, this model is valid only for the experimental results of current study at present. In the further study, more tests will be conducted to proving the veracity of this model.

## 5 Conclusions

In this study, the four-point bending tests were carried out for NAPC and RAPC to investigate the fatigue mechanics characteristics of the two pervious concrete specimens. Besides, the simplified fatigue model was proposed to predict the fatigue life of NAPC and RAPC under four different stress levels.

1. The area of the hysteresis loop and the damping ratio increased with the increases of the stress levels and the loading cycles. And the damping ratio of RAPC was higher than that of NAPC.
2. Under cyclic loading, the dynamic elastic modulus, the total strain and the plastic strain of the pervious concrete specimens exhibited the three-stage trend.
3. According to the experimental data of loading–unloading test, the formulas of the fracture parameter and the plastic strain of pervious concrete were obtained. And the relationship between the loading cycles and the ratio of the plastic strain to the unloading strain was built.
4. The simplified fatigue model was proposed, which can effectively evaluate the variation of total strain, plastic strain and fracture parameter, and predict the fatigue life of pervious concrete specimens at different stress levels.
5. The experimental results were verified by the proposed model. The fitting result reached a good agreement.

**Abbreviations**

RAPC: Recycled aggregate pervious concrete; NAPC: Natural aggregate pervious concrete.

**Authors' contributions**

The authors built the relationships between fracture parameters, plastic strain and unloading strain. The static stress–strain models of two kinds of pervious concrete were given and the relationship between the loading cycles and the ratio of plastic strain and unloading strain was given in this paper. Further, the simplified fatigue model of pervious concrete was proposed. All authors read and approved the final manuscript.

**Acknowledgements**

This research is based upon work support supported by the National Natural Science Foundation of China (Grant No. 51779085), the Natural Science Foundation of Jiangsu Province (Grant No. BK20150820) and the Young Elite Scientists Sponsorship Program by China Association for Science and Technology (No. 2017QNRC001) granted to the first author Xudong Chen.

**Competing interests**

The authors declare that they have no competing interests.

**Availability of data and materials**

The data and materials are available.

**Consent for publication**

The authors consent for publication.

**Ethics approval and consent to participate**

The authors state that the research was conducted according to ethical standards.

**Funding**

Not applicable.

## Publisher's Note



Received: 10 March 2018 Accepted: 27 September 2018
Published online: 28 January 2019

**References**

Arora, S., & Singh, S. P. (2016). Analysis of flexural fatigue failure of concrete made with 100% coarse recycled concrete aggregates. *Construction and Building Materials, 102,* 782–791.

Barnhouse, P. W., & Srubar, W. V., III. (2016). Material characterization and hydraulic conductivity modeling of macroporous recycled-aggregate pervious concrete. *Construction and Building Materials, 110,* 89–97.

Bhutta, M. A. R., Hasanah, N., Farhayu, N., Hussin, M. W., bin Md, W., Tahir, M., et al. (2013). Properties of porous concrete from waste crushed concrete (recycled aggregate). *Construction and Building Materials, 47,* 1243–1248.

Chandrappa, A. K., & Biligiri, K. P. (2016). Pervious concrete as a sustainable pavement material–Research findings and future prospects: a state-of-the-art review. *Construction and Building Materials, 111,* 262–274.

Chen, X., Huang, Y., Chen, C., Lu, J., & Fan, X. (2017). Experimental study and analytical modeling on hysteresis behavior of plain concrete in uniaxial cyclic tension. *International Journal of Fatigue, 96,* 261–269.

Ćosić, K., Korat, L., Ducman, V., & Netinger, I. (2015). Influence of aggregate type and size on properties of pervious concrete. *Construction and Building Materials, 78,* 69–76.

El-Kashif, K. F., & Maekawa, K. (2004). Time-dependent nonlinearity of compression softening in concrete. *Journal of Advanced Concrete Technology, 2*(2), 233–247.

Fu, T. C., Huang, R., Yeih, W. C., Chang, J. J., & Lee, P. C. (2015). Study of the pervious concrete properties using the experimental design method. *Advanced Materials Research, 1089,* 253–264.

Güneyisi, E., Gesoğlu, M., Kareem, Q., & İpek, S. (2016). Effect of different substitution of natural aggregate by recycled aggregate on performance characteristics of pervious concrete. *Materials and Structures, 49*(1–2), 521–536.

Heeralal, M., Kumar, R. P., & Rao, Y. V. (2009). Flexural fatigue characteristics of steel fiber reinforced recycled aggregate concrete (SFRRAC). *Architecture and Civil Engineering, 7*(1), 19–33.

Joshaghani, A., Ramezanianpour, A. A., Ataei, O., & Golroo, A. (2015). Optimizing pervious concrete pavement mixture design by using the Taguchi method. *Construction and Building Materials, 101,* 317–325.

Li, H., & Yu, B. (2014). Fatigue performance and prediction model of multilayer deck pavement with different tack coat materials. *Journal of Materials in Civil Engineering, 26*(5), 872–877.
Maekawa, K., & Okamura, H. (1983). The deformational behavior and constitutive equation of concrete using elasto-plastic and fracture model. *Journal of the Faculty of Engineering, 37*(2), 253–328.
Maekawa, K., Toongoenthong, K., Gebreyouhannes, E., & Kishi, T. (2006). Direct path-integral scheme for fatigue simulation of reinforced concrete in shear. *Journal of Advanced Concrete Technology, 4*(1), 159–177.
Mannan, U. A., Islam, M. R., & Tarefder, R. A. (2015). Effects of recycled asphalt pavements on the fatigue life of asphalt under different strain levels and loading frequencies. *International Journal of Fatigue, 78,* 72–80.
Qin, Y., Yang, H., Deng, Z., & He, J. (2015). Water permeability of pervious concrete is dependent on the applied pressure and testing methods. *Advances in Materials Science and Engineering, 404136,* 1–6.
Senaratne, S., Gerace, D., Mirza, O., Tam, V. W., & Kang, W. H. (2016). The costs and benefits of combining recycled aggregate with steel fibres as a sustainable, structural material. *Journal of Cleaner Production, 112,* 2318–2327.
Sriravindrarajah, R., Wang, N. D. H., & Ervin, L. J. W. (2012). Mix design for pervious recycled aggregate concrete. *International Journal of Concrete Structures and Materials, 6*(4), 239–246.
Sumanasooriya, M. S., & Neithalath, N. (2011). Pore structure features of pervious concretes proportioned for desired porosities and their performance prediction. *Cement and Concrete Composites, 33*(8), 778–787.
Thomas, C., Setién, J., Polanco, J. A., Lombillo, I., & Cimentada, A. (2014a). Fatigue limit of recycled aggregate concrete. *Construction and Building Materials, 52*(2), 146–154.
Thomas, C., Sosa, I., Setién, J., Polanco, J. A., & Cimentada, A. I. (2014b). Evaluation of the fatigue behavior of recycled aggregate concrete. *Journal of Cleaner Production, 65,* 397–405.
Xiao, J., Li, H., & Yang, Z. (2013). Fatigue behavior of recycled aggregate concrete under compression and bending cyclic loadings. *Construction and Building Materials, 38*(2), 681–688.
Yang, J., & Jiang, G. (2003). Experimental study on properties of pervious concrete pavement materials. *Cement and Concrete Research, 33*(3), 381–386.
Yehia, S., Helal, K., Abusharkh, A., Zaher, A., & Istaitiyeh, H. (2015). Strength and durability evaluation of recycled aggregate concrete. *International Journal of Concrete Structures and Materials, 9*(2), 219–239.
Zaetang, Y., Sata, V., Wongsa, A., & Chindaprasirt, P. (2016). Properties of pervious concrete containing recycled concrete block aggregate and recycled concrete aggregate. *Construction and Building Materials, 111,* 15–21.
Zhang, Z., Zhang, Y., Yan, C., & Liu, Y. (2017). Influence of crushing index on properties of recycled aggregates pervious concrete. *Construction and Building Materials, 135,* 112–118.